CORRECTED 10 DECEMBER 2014; SEE ERRATUM

RESEARCH ARTICLE

BLOOD-BRAIN BARRIER

# The gut microbiota influences blood-brain barrier permeability in mice

Viorica Braniste,[1]*† Maha Al-Asmakh,[1]* Czeslawa Kowal,[2]* Farhana Anuar,[1] Afrouz Abbaspour,[1] Miklós Tóth,[3] Agata Korecka,[1] Nadja Bakocevic,[4] Lai Guan Ng,[4] Parag Kundu,[5] Balázs Gulyás,[3,5] Christer Halldin,[3,5] Kjell Hultenby,[6] Harriet Nilsson,[7] Hans Hebert,[7] Bruce T. Volpe,[8] Betty Diamond,[2‡] Sven Pettersson[1,5,9†‡]

**Pivotal to brain development and function is an intact blood-brain barrier (BBB), which acts as a gatekeeper to control the passage and exchange of molecules and nutrients between the circulatory system and the brain parenchyma. The BBB also ensures homeostasis of the central nervous system (CNS). We report that germ-free mice, beginning with intrauterine life, displayed increased BBB permeability compared to pathogen-free mice with a normal gut flora. The increased BBB permeability was maintained in germ-free mice after birth and during adulthood and was associated with reduced expression of the tight junction proteins occludin and claudin-5, which are known to regulate barrier function in endothelial tissues. Exposure of germ-free adult mice to a pathogen-free gut microbiota decreased BBB permeability and up-regulated the expression of tight junction proteins. Our results suggest that gut microbiota–BBB communication is initiated during gestation and propagated throughout life.**

## INTRODUCTION

Our gut microbiota is important for many biological functions in the body, including intestinal development, barrier integrity and function (*1*, *2*), metabolism (*3*, *4*), the immune system (*5*), and the central nervous system (CNS). The effects of the gut microbiota on brain physiology include synaptogenesis, regulation of neurotransmitters and neurotrophic factors such as brain-derived neurotrophic factor and nerve growth factor-A1 (*6*). However, the development of the CNS also includes the formation of an intact blood-brain barrier (BBB) that ensures an optimal microenvironment for neuronal growth and specification (*7*). An intact and tightly regulated BBB is also required to protect against colonizing microbiota in neonates during the critical period of brain development (*8*, *9*). It also protects against exposure to "new" molecules and bacterial metabolites due to the postnatal metabolic switch from predominant dependence on carbohydrates during fetal life to a greater dependence on fatty acid catabolism after birth.

The BBB begins to develop during the early period of intrauterine life (*10*, *11*) and is formed by capillary endothelial cells sealed by tight junctions, astrocytes, and pericytes. Tight junction proteins restricting paracellular diffusion of water-soluble substances from blood to the brain (*12*) consist mainly of transmembrane proteins such as claudins, tricellulin, and occludin, which are connected to the actin cytoskeleton by the zona occludens (ZO-1) (*13*). Tight junction proteins are dynamic structures and are subject to changes in expression, subcellular location, posttranslational modification, and protein-protein interactions under both physiological and pathophysiological conditions (*12*). Disruption of tight junctions due to disease or drugs can lead to impaired BBB function, compromising the CNS. Therefore, understanding how BBB tight junction proteins are affected by various factors is important for elucidating how to prevent and treat neurological diseases.

Here, we report that the intestinal microbiota affects BBB permeability in both the fetal and adult mouse brain. Using as a model system germ-free mice that have never encountered a live bacterium and pathogen-free mice that were reared in an environment free of monitored mouse pathogens, we demonstrated that lack of gut microbiota is associated with increased BBB permeability and altered expression of tight junction proteins. Fecal transfer from mice with pathogen-free gut flora into germ-free mice or treatment of germ-free mice with bacteria that produce short chain fatty acids (SCFA) decreased the permeability of the BBB.

## RESULTS

### The maternal gut microbiota can influence prenatal development of the BBB

First, we characterized BBB permeability of mouse embryos with pathogen-free mothers by administering infrared-labeled immunoglobulin G2b (IgG2b) antibody to dams during timed pregnancies to see whether the antibody was excluded by the BBB or was able to cross the BBB into the brain parenchyma. The qualitative analysis of mouse embryos with pathogen-free mothers showed a shift from a diffuse infrared-labeled antibody signal present within the embryonic brain at E13.5 and E14.5 to a signal confined to the developing vasculature starting at E15.5 to E17.5 (Fig. 1A). This signal was most pronounced in adult offspring of pathogen-free dams (Fig. 1A). The quantitative analysis of the penetration into the fetal brain of infrared-labeled IgG2b antibody injected

[1]Department of Microbiology, Tumor and Cell Biology, Karolinska Institute, 17177 Stockholm, Sweden. [2]Center for Autoimmune and Musculoskeletal Disease, The Feinstein Institute for Medical Research, North Shore-LIJ Health System, Manhasset, NY 11030, USA. [3]Psychiatry Section, Department of Clinical Neuroscience, Karolinska Institutet, 17176 Stockholm, Sweden. [4]Singapore Immunology Network, Agency for Science, Technology and Research, Singapore 138648, Singapore. [5]Lee Kong Chian School of Medicine, Nanyang Technological University, 60 Nanyang Drive, Singapore 637551, Singapore. [6]Department of Laboratory Medicine, Karolinska Institutet, 14186 Stockholm, Sweden. [7]Department of Biosciences and Nutrition, Karolinska Institutet, and School of Technology and Health, KTH Royal Institute of Technology, Novum, SE-141 57 Huddinge, Sweden. [8]Laboratory of Functional Neuroanatomy, The Feinstein Institute for Medical Research, North Shore-LIJ Health System, Manhasset, NY 11030, USA. [9]Singapore Centre on Environmental Life Sciences Engineering (SCELSE), Nanyang Technological University, Singapore 637551, Singapore.
*Co-first authors.
†Corresponding author. E-mail: viorica.braniste@ki.se (V.B.); sven.pettersson@ki.se (S.P.)
‡Co-senior authors.

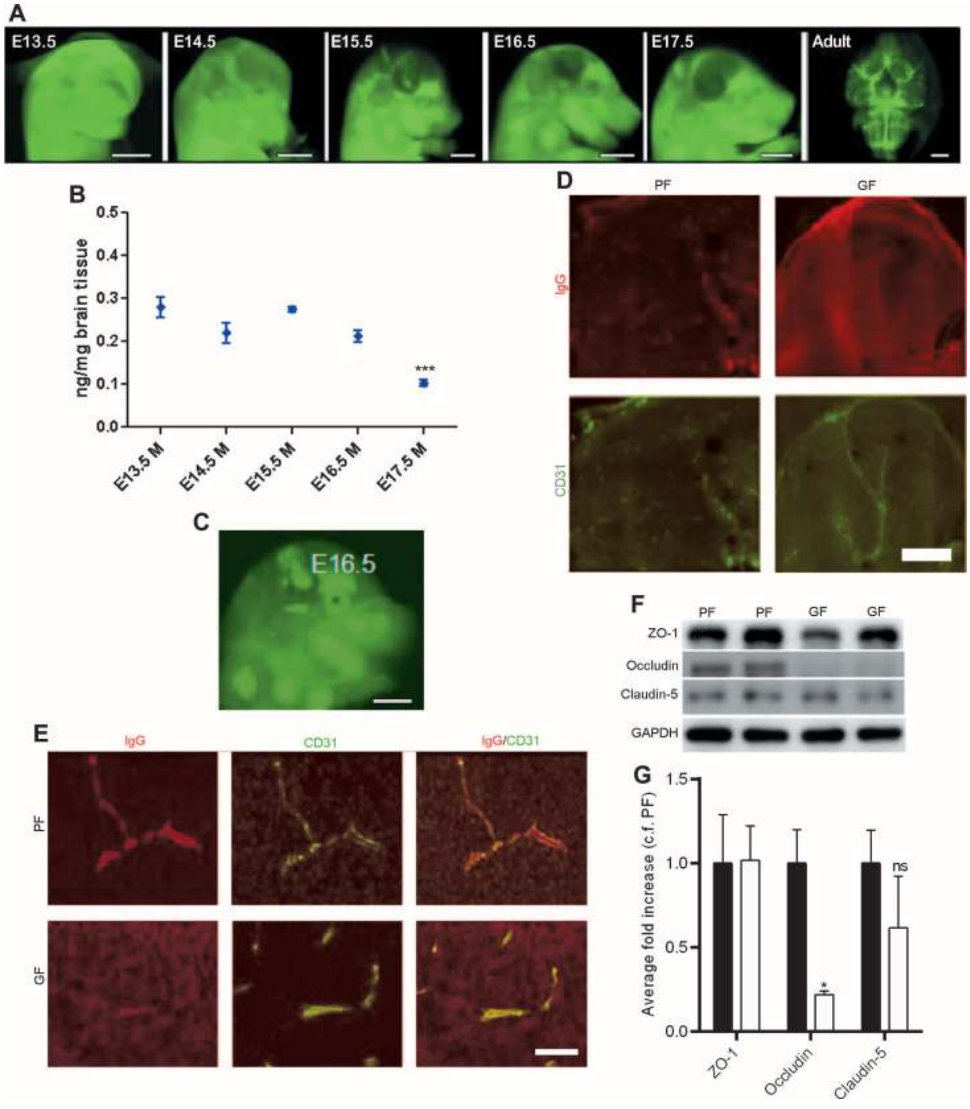


**Fig. 1. BBB integrity in fetal mice with germ- or pathogen-free mothers.** (**A**) Representative lateral images of the brains of E13.5 to E17.5 mouse embryos and adult mice (ventral) 1 hour after infrared-labeled antibody was injected into pregnant pathogen-free (PF) mothers. Scale bar, 1 mm. (**B**) Quantitative analysis of antibody penetration into the fetal brain of mice with pathogen-free mothers. Data are expressed as means ± SEM (7 to 12 embryos per group). ***$P < 0.0001$ between E17.5 group versus the rest of the groups by one-way analysis of variance (ANOVA). (**C**) Representative images from the infrared-labeled antibody assay in E16.5 mouse embryos with germ-free (GF) mothers. Scale bar, 1 mm. (**D**) Sagittal brain sections from each of three E16.5 mouse embryos with germ- or pathogen-free mothers after injecting the dam with IgG. IgG (top row of each pair, Alexa 594), CD31 [platelet endothelial cell adhesion molecule (PECAM); bottom row of each pair, Alexa 488]. Scale bar, 500 μm. (**E**) Maternal IgG in comparable regions of the brain of E16.5 mouse embryos. Left column: IgG (Alexa 594). Middle column: CD31 (PECAM; Alexa 488). Right column: Merged images. Scale bar, 20 μm. (**F** and **G**) Western blots of brain lysates from E18.5 mouse fetuses with germ- or pathogen-free mothers probed for ZO-1, occludin, claudin-5, and glyceraldehyde phosphate dehydrogenase (GAPDH) (control). (F) Representative blots and (G) quantification. Black bars, PF. White bars, GF. Data were normalized for GAPDH expression and expressed as fold change, control fold (c.f.) PF. Data are means ± SEM (four to six mice per group). *$P < 0.05$ by Student's *t* test. ns, not significant.

intravenously into pathogen-free dams supported the qualitative data, showing a decrease at E15.5 to E17.5 (Fig. 1B). In contrast, the analysis of E16.5 brains from fetal mice of germ-free dams showed a diffuse signal from the infrared-labeled IgG2b antibody (Fig. 1C) present in the brain parenchyma (Fig. 1, D and E). Higher-magnification images of the brain showed that the IgG2b antibody was limited only to the vessels in E16.5 fetal mice of pathogen-free dams in contrast to age-matched fetal mice of germ-free dams (Fig. 1, D and E). Because BBB integrity is controlled in part by sealing of the endothelial cells via tight junctions, we determined expression of the main tight junction proteins in brain lysates from E18.5 fetal mice of pathogen-free versus germ-free dams. Expression of the brain endothelial tight junction proteins claudin-5 and ZO-1 was similar between the two groups, whereas the expression of occludin was significantly lower in the brain lysates from E18.5 fetal mice of germ-free dams compared to that in age-matched fetal mice of pathogen-free dams ($P < 0.05$) (Fig. 1, F and G).

### Lack of gut microbiota is associated with increased BBB permeability in adult mice

Three techniques were used to determine whether the BBB was more permeable in germ-free adult mice: (i) in vivo positron emission tomography (PET) imaging with [$^{11}$C]raclopride (Fig. 2, A to C); (ii) extravasation of Evans blue tracer from the circulation (Fig. 2D); and (iii) the capacity of an anti–*N*-methyl-D-aspartate receptor reactive antibody (R4A) to induce neuronal death after intravenous administration (Fig. 2, E and F).

In germ-free adult mice, [$^{11}$C]raclopride uptake was increased compared with that for pathogen-free adult mice (Fig. 2A), but only during the first 4 min after injection (Fig. 2, B and C). This period of time represents the "flow phase" (that is, the presence of the radioligand in the whole brain due to BBB permeability). Because the radioligand was given in tracer doses, it does not exert any pharmacological effects on the brain (or body) vasculature or heart rate. These differences were present only in the initial flow phase and not in the later phase of the time activity curves, indicating no differences in radioligand binding to dopamine $D_2$ receptors between the groups.

Fluorescence microscopy images of different brain regions (cortex, striatum, and hippocampus) of pathogen-free adult mice showed the presence of Evans blue dye (bright red) only in the blood vessels, whereas Evans blue staining in germ-free mice was detected not only in the blood vessels but also in the brain parenchyma, demonstrating leakage of the dye across the BBB (Fig. 2D). A group of mice receiving an intravenous

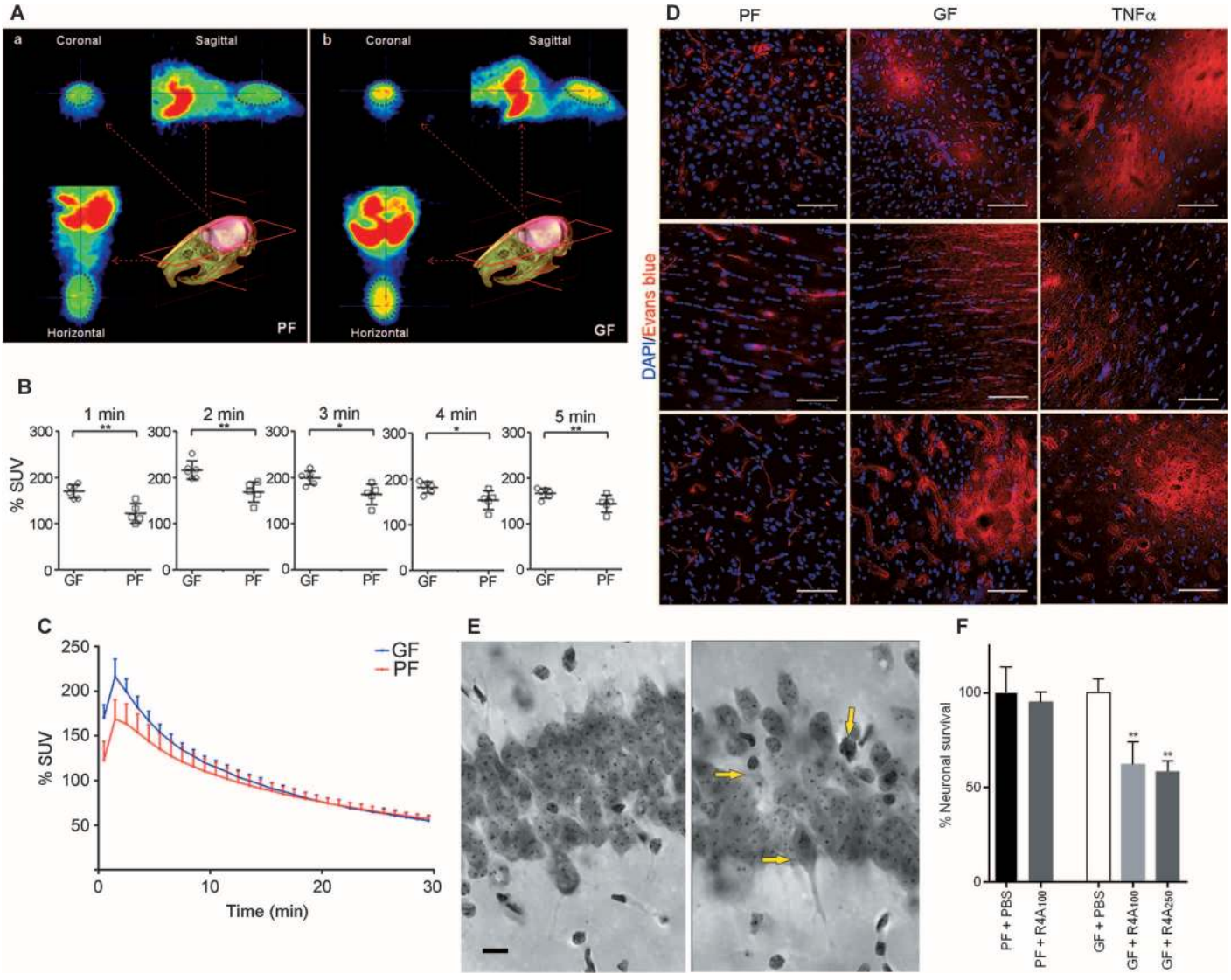


**Fig. 2. Increased BBB permeability in adult germ-free versus pathogen-free mice.** (**A**) In vivo PET imaging of [$^{11}$C]raclopride. Average coronal, sagittal, and horizontal PET summation images (brain area encircled in purple ellipse) in pathogen-free (PF) or germ-free (GF) adult mice 2 to 3 min after [$^{11}$C]raclopride injection. (**B**) Average whole-brain time-activity curves of [$^{11}$C] raclopride uptake expressed as % standardized uptake value (% SUV) in the two groups. *$P < 0.05$ and **$P < 0.05$ by one-way ANOVA. (**C**) Values (% SUV) obtained at 1-min intervals during the first 5 min. Data are expressed as means ± SEM (five to six mice per group). (**D**) Representative images showing Evans blue dye extravasation (red) in three brain regions (cortex - upper row, striatum - middle row, and hippocampus - lower row) of germ- and pathogen-free mice and pathogen-free mice treated with TNFα ($n = 3$ mice per group). Blue, 4′,6-diamidino-2-phenylindole (DAPI) (nuclear staining). Scale bar, 50 μm. (**E** and **F**) Neuronal loss in the hippocampus of germ-free adult mice receiving R4A antibody. (E) Photomicrographs of the CA1 region of the hippocampus (middorsal, matched sections) from PBS-treated germ-free adult mice (left) and germ-free mice treated with different concentrations of R4A antibody (100 and 250 μg) (right). Yellow arrows in the right panel indicate neuronal loss and dying neurons in R4A-treated germ-free mice. Scale bar, 10 μm. (F) Quantitative analysis. Percent neuronal survival in the PBS-treated germ-free mouse group was set at 100%. **$P < 0.01$ by one-way ANOVA compared with the PBS-treated germ-free mouse group ($n = 3$ mice per group).

injection of tumor necrosis factor–α (TNFα) 15 hours before the experiment served as a positive control for BBB leakiness (Fig. 2D).

In germ-free adult mice, intravenous administration of the monoclonal antibody R4A (250 μg) was associated with abnormal neurons, marked by condensed cytoplasm and shrunken cell bodies in the CA1 region of the hippocampus (Fig. 2E, right panel). Abnormal neurons were not present or were rare in the CA1 region of the hippocampus in the control group [phosphate-buffered saline (PBS)–treated germ-free group; Fig. 2E, left panel]. Furthermore, the R4A injection (at low and high doses) in germ-free adult mice was associated with a significant reduction in neuron numbers in the CA1 region of the hippocampus, –38% for low-dose R4A (100 μg) and –42% for high-dose (250 μg) R4A compared with the PBS-treated germ-free control group ($P < 0.01$) (Fig. 2F). Intravenous administration of R4A in pathogen-free adult mice did not induce any changes, indicating that the R4A monoclonal antibody did not penetrate the BBB (Fig. 2F).

### Vascular density and pericyte coverage show no difference in germ- and pathogen-free adult mice

We used intravital two-photon microscopy to exclude the possibility that high BBB permeability in germ-free adult mice was caused by higher vascular density in the brain. Using the second harmonic generation signals from collagen fibers of dura mater as a reference point, we observed that the subdural region, which is 20 to 80 μm below the dura mater, contains mainly large vessels (average diameter, ~40 μm) (Fig. 3, A and C). In contrast, deeper regions of the brain 120 to 180 μm below the dura mater consist mostly of capillaries (Fig. 3, B and D). Quantitative analysis of vasculature density in the brain revealed no significant gross differences between germ- and pathogen-free adult mice (Fig. 3, C and D).

Pericytes play an important role in regulating BBB properties, and decreased pericyte coverage has been associated with increased BBB permeability (*10*, *14*). Immunofluorescence staining using CD13, a cell surface marker for pericytes in different brain regions, revealed no difference in pericyte coverage between germ- and pathogen-free mice (Fig. 3E).

### Brain endothelial tight junctions are altered in the absence of a gut microbiota

Permeability of CNS vessels is controlled in part by dynamic opening and closing of the endothelial junctions (*15*). Therefore, we assessed the expression of the main tight junction proteins (ZO-1, occludin, and claudin-5) by Western blot in three regions of an adult mouse brain: frontal cortex, striatum, and hippocampus. Significantly lower expression of occludin and claudin-5 was observed in male germ-free mice compared with male pathogen-free mice in all three brain regions of interest (occludin: $P < 0.001$ in frontal cortex and hippocampus and $P < 0.05$ in striatum; claudin-5: $P > 0.001$ in frontal cortex and $P < 0.01$ in striatum and hippocampus) (Fig. 4, A to F). In contrast, no difference in the expression of the cytoplasmic protein ZO-1 was observed between the two groups (Fig. 4, A to F). Similar patterns of tight junction protein expression were observed in the brains of female germ-free mice compared with female pathogen-free mice (fig. S1), suggesting that the effect of gut microbiota on the integrity of the BBB is independent of sex. In addition, immunofluorescence analysis confirmed lower expression of occludin and claudin-5 in the brain vessels of adult male germ-free mice compared with that of adult male pathogen-free mice (Fig. 4, G and H).

The ultrastructure of the tight junctions was investigated by transmission electron microscopy analysis. In germ-free adult mice, the tight junctions appeared as a diffuse, disorganized structure compared with those in the pathogen-free group (Fig. 4I). A scoring system was used to quantitatively determine the number of intact tight junctions as follows: perfect tight junctions, 3; patches of blurriness, 2; totally blurred, 1 (fig. S2 shows examples of the rating scale). In the striatum of germ-free adult mice, the number of intact tight junctions was significantly lower than that in pathogen-free mice ($P < 0.001$) (Fig. 4J).

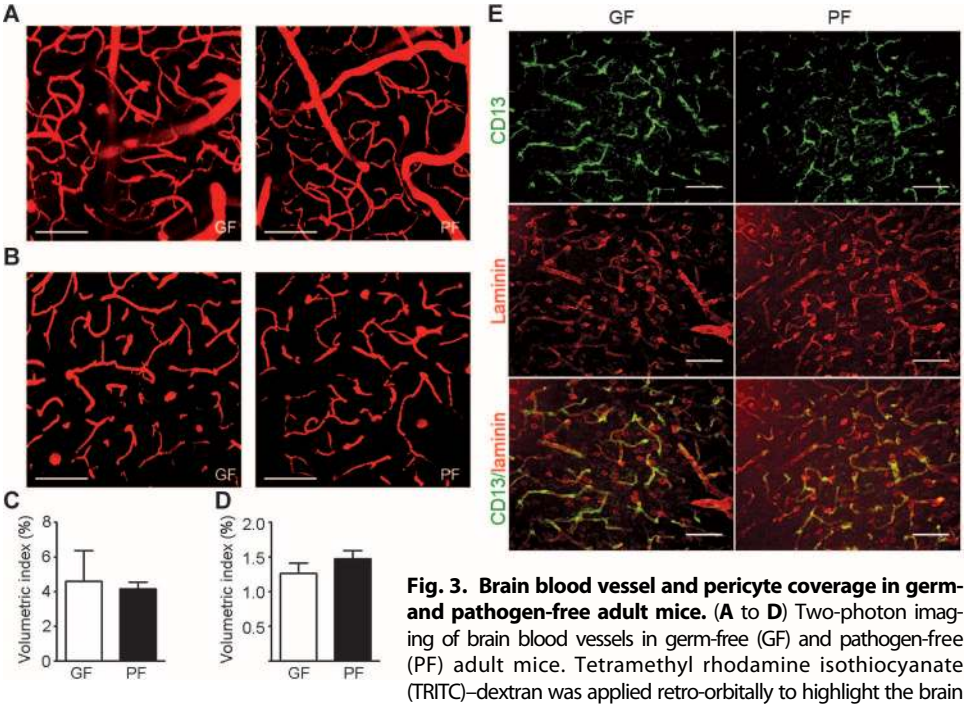


**Fig. 3. Brain blood vessel and pericyte coverage in germ- and pathogen-free adult mice.** (**A** to **D**) Two-photon imaging of brain blood vessels in germ-free (GF) and pathogen-free (PF) adult mice. Tetramethyl rhodamine isothiocyanate (TRITC)–dextran was applied retro-orbitally to highlight the brain blood vessels. (A) Representative images of brain vasculature 20 to 80 μm below the dura mater in germ-free (left panel) and pathogen-free (right panel) mice reveal mainly large vessels (average diameter, ~40 μm). (B) Representative images of the brain vasculature 120 to 180 μm below the dura mater in germ-free (left panel) and pathogen-free (right panel) mice showing mainly capillaries. (C) Quantitative analysis of blood vessel density 20 to 80 μm below the dura mater. (D) Quantitative analysis of blood vessel density 120 to 180 μm below the dura mater. Scale bars, 100 μm. Data are representative of $n = 3$ independent experiments. (**E**) Representative images of pericyte coverage (CD13, green) in the cerebral cortex of pathogen- and germ-free mice ($n = 4$ mice per group). Laminin (red) was used as an endothelial cell marker. Scale bars, 50 μm.

### BBB permeability and tight junction protein expression are associated with changes in the gut microbiota

Colonization of germ-free adult mice with flora from pathogen-free mice [conventionalized (CONV)] was associated with increased integrity of the BBB as shown by restriction of the Evans blue tracer to the blood vessels and decreased extravasation of the dye into the brain parenchyma (Fig. 5A). Quantitative analysis of tight junction proteins in the CONV group compared with germ-free mice showed a significant increase in the expression of occludin in the frontal cortex ($P < 0.05$) and striatum ($P = 0.05$) and of claudin-5 in the hippocampus and striatum ($P < 0.05$) (Fig. 5, B to G). Increased expression of the intracellular protein ZO-1 was detected in the striatum and hippocampus of CONV mice compared with germ-free controls ($P < 0.05$) (Fig. 5, B to G).

### SCFAs or metabolites produced by bacteria affect BBB permeability

SCFAs are known to enhance the integrity of the intestinal epithelial barrier (*16*, *17*) by facilitating the assembly of tight junctions

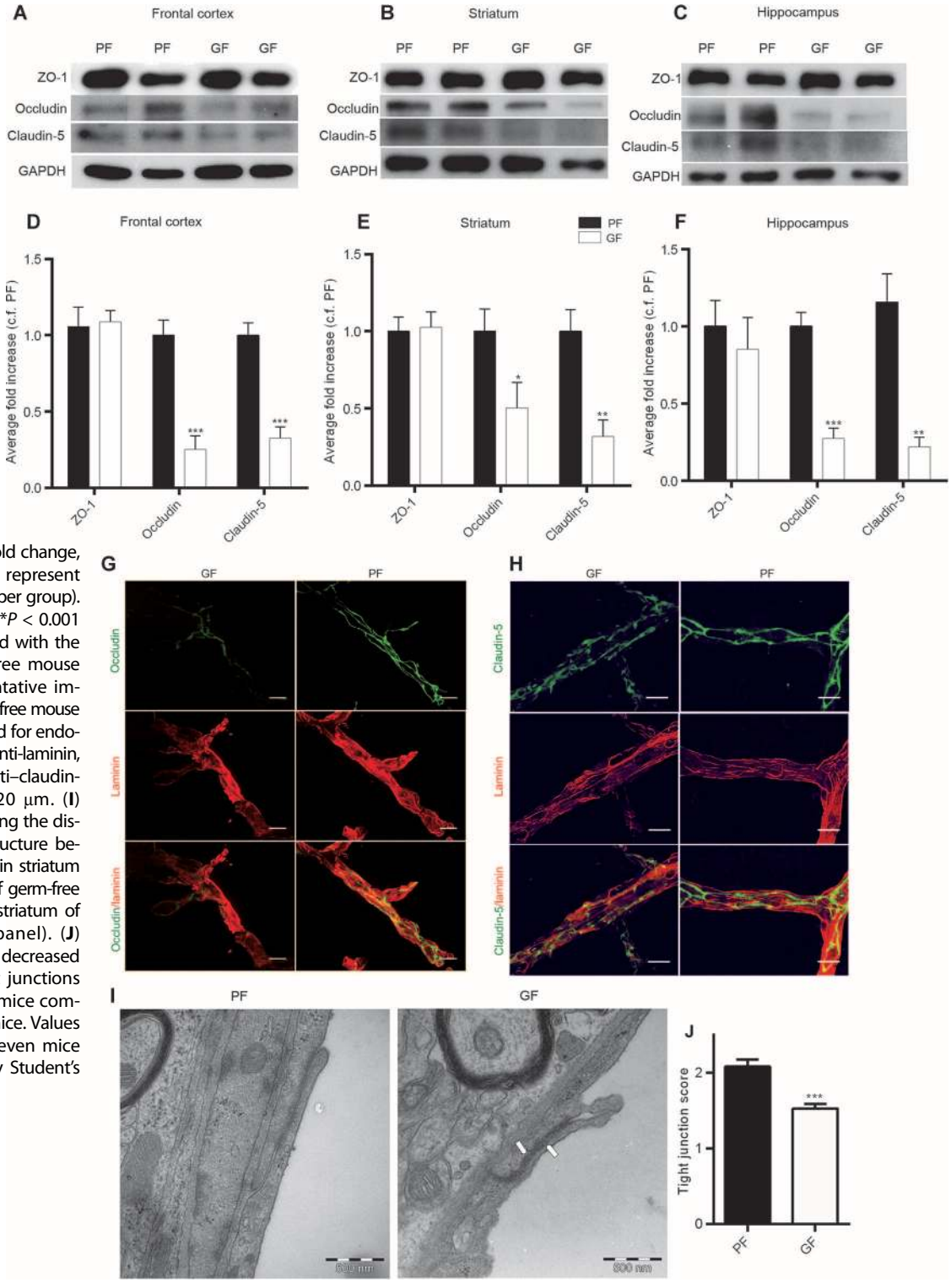


**Fig. 4. Disrupted BBB tight junctions in the brains of germ- and pathogen-free adult mice.** (**A** to **C**) Representative Western blots showing the expression of ZO-1, occludin, and claudin-5 in the (A) frontal cortex, (B) striatum, and (C) hippocampus of germ-free (GF) and pathogen-free (PF) adult mice. (**D** to **F**) Densitometric analysis of Western blots from protein samples of the (D) frontal cortex, (E) striatum, and (F) hippocampus of germ-free mice (white bars) compared with pathogen-free mice (black bars). Data were normalized for GAPDH expression and expressed as fold change, control fold (c.f.) PF. Values represent means ± SEM (6 to 10 mice per group). $^{*}P < 0.05$, $^{**}P < 0.01$, and $^{***}P < 0.001$ by Student's *t* test compared with the corresponding pathogen-free mouse control. (**G** and **H**) Representative images of germ- and pathogen-free mouse cerebral motor cortex stained for endothelial cells with (G and H) anti-laminin, (G) anti-occludin, and (H) anti–claudin-5 antibodies. Scale bars, 20 μm. (**I**) Electron micrographs showing the disorganized tight junction structure between two endothelial cells in striatum (right panel, white arrows) of germ-free adult mice compared with striatum of pathogen-free mice (left panel). (**J**) Quantitative data indicate a decreased number of organized tight junctions in the striatum of germ-free mice compared with pathogen-free mice. Values represent means ± SEM (seven mice per group). $^{***}P < 0.001$ by Student's *t* test.

(*18*). Hence, we evaluated BBB permeability in germ-free adult mice monocolonized with a single bacterial strain, *Clostridium tyrobutyricum* (CBut), that produces mainly butyrate (*19*, *20*) or with *Bacteroides thetaiotaomicron* (BTeta), which produces mainly acetate and propionate (*21*, *22*). We also evaluated germ-free adult mice given sodium butyrate by oral gavage for 3 days. Evans blue perfusion in CBut-, BTeta-, and sodium butyrate–treated mice demonstrated decreased BBB permeability, compared to that in germ-free adult mice, that was equivalent to that of pathogen-free adult mice (Fig. 6A). Administration of sodium butyrate to germ-free mice was associated with increased expression of

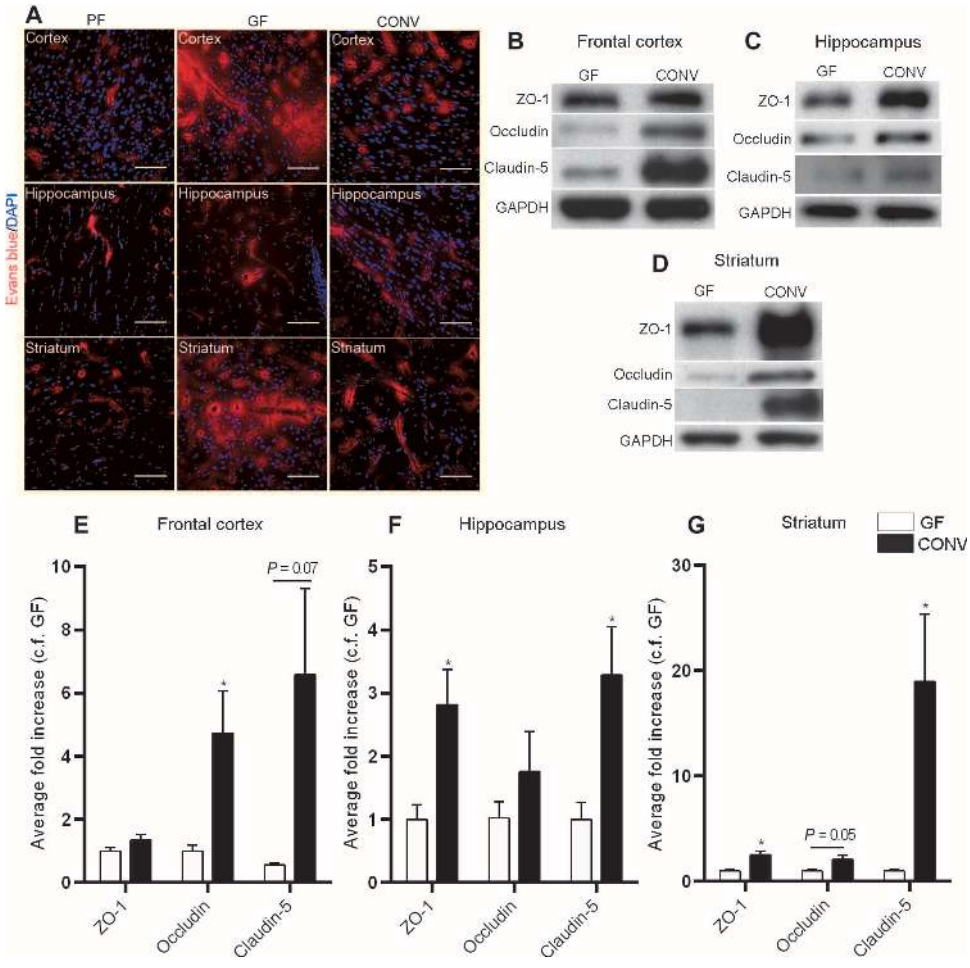


**Fig. 5. Microbial colonization of the gut changes BBB integrity.** (**A**) Representative images from three mouse brain regions (frontal cortex, striatum, and hippocampus) showing Evans blue dye (red) in pathogen-free (PF) mice, germ-free (GF) mice, and germ-free mice colonized with pathogen-free flora for 14 days (CONV). Blue, DAPI (nuclear staining). Scale bars, 50 μm. (**B** to **G**) Quantitative analysis of ZO-1, occludin, and claudin-5 expression in the frontal cortex, striatum, and hippocampus of germ-free and CONV mice. Data were normalized for GAPDH expression and expressed as fold change, fold control (c.f.) GF. Values represent means ± SEM (four to six mice per group). *$P < 0.05$ by Student's $t$ test compared to the germ-free control.

occludin in the frontal cortex and hippocampus but had no effect on the expression of claudin-5 (Fig. 6, B to D). Furthermore, administration of sodium butyrate or monocolonization of germ-free mice with *C. tyrobutyricum* was associated with an increase in histone acetylation in brain lysates (fig. S3).

## DISCUSSION

The BBB is a physiological barrier that controls the passage of molecules between the brain parenchyma and the blood and in so doing allows proper functioning of neurons. Our results highlight the gut microbiota as a potential regulator of BBB integrity. Here, we show that the lack of a normal gut microbiota in germ-free mice is associated with increased permeability of the BBB. This result was confirmed using three different techniques: in vivo PET imaging using radiolabeled ligand, vascular leakage of Evans blue dye, and neuronal damage after intravenous administration of R4A antibody. Furthermore, our data show that a more permeable BBB is observed in the fetal mice with germ-free mothers at E16.5 to E18.5 days of embryonic development compared to the fetal mice with pathogen-free mothers at the same stages of development. The increased permeability of the BBB in germ-free adult mice may partly be the consequence of disorganized tight junctions, as shown by electron microscopy analysis, and low expression of the transmembrane tight junction proteins occludin and claudin-5. The "conventionalization" of germ-free adult mice through transplant of the fecal microbiota from pathogen-free adult mice or by administering bacterial strains that produce SCFAs reinforced the integrity of the mouse BBB.

The BBB matures progressively during intrauterine life and continues to mature during the early postnatal stages of life (*23*). Our data confirm previous observations (*10*, *24*) and show that closure of the BBB to IgG in pathogen-free mice occurs during the later stages of intrauterine life. A recent study of Mfsd2a knockout mice (lacking the transporter for the essential omega-3 fatty acid docosahexaenoic acid) showed that the BBB in mice becomes functional at E15.5, demonstrating complex regional and temporal differences in maturation (*11*). This coincides with our observation of the permeability of the embryonic BBB to maternal antibodies. In mice, gestational stage E15.5 is a turning point for the restriction of maternal antibody penetration into the fetal brain. Maternal antibodies or, more precisely, antibody delivered to the embryo through the placenta was our molecule of choice in our embryonic BBB studies as a physiological route of delivery. Reduced closure of the BBB was observed in fetuses from germ-free dams. In humans, marked changes in the composition of the maternal gut microbiota have been observed between the first and the third trimesters of pregnancy (*25*). These observations, together with the present study, imply that the maternal gut microbiota might contribute to increased nutritional demands in late pregnancy, which would require more stringent control of BBB permeability in the growing offspring.

The BBB is a complex structure formed by capillary endothelial cells, pericytes, and astrocytes (*26*). A difference in vascular density might be a confounding factor in assessing BBB permeability. In our study, increased invasion of circulating substances into the brain parenchyma appears not to be due to differences in large vascular structures between the two groups of mice as shown by a comparable equal visualization of the brain vasculature using 140 kD TRITC-dextran. However, we cannot formally exclude that some microcapillary changes may still exist between the two groups. In germ-free adult mice, pericyte coverage

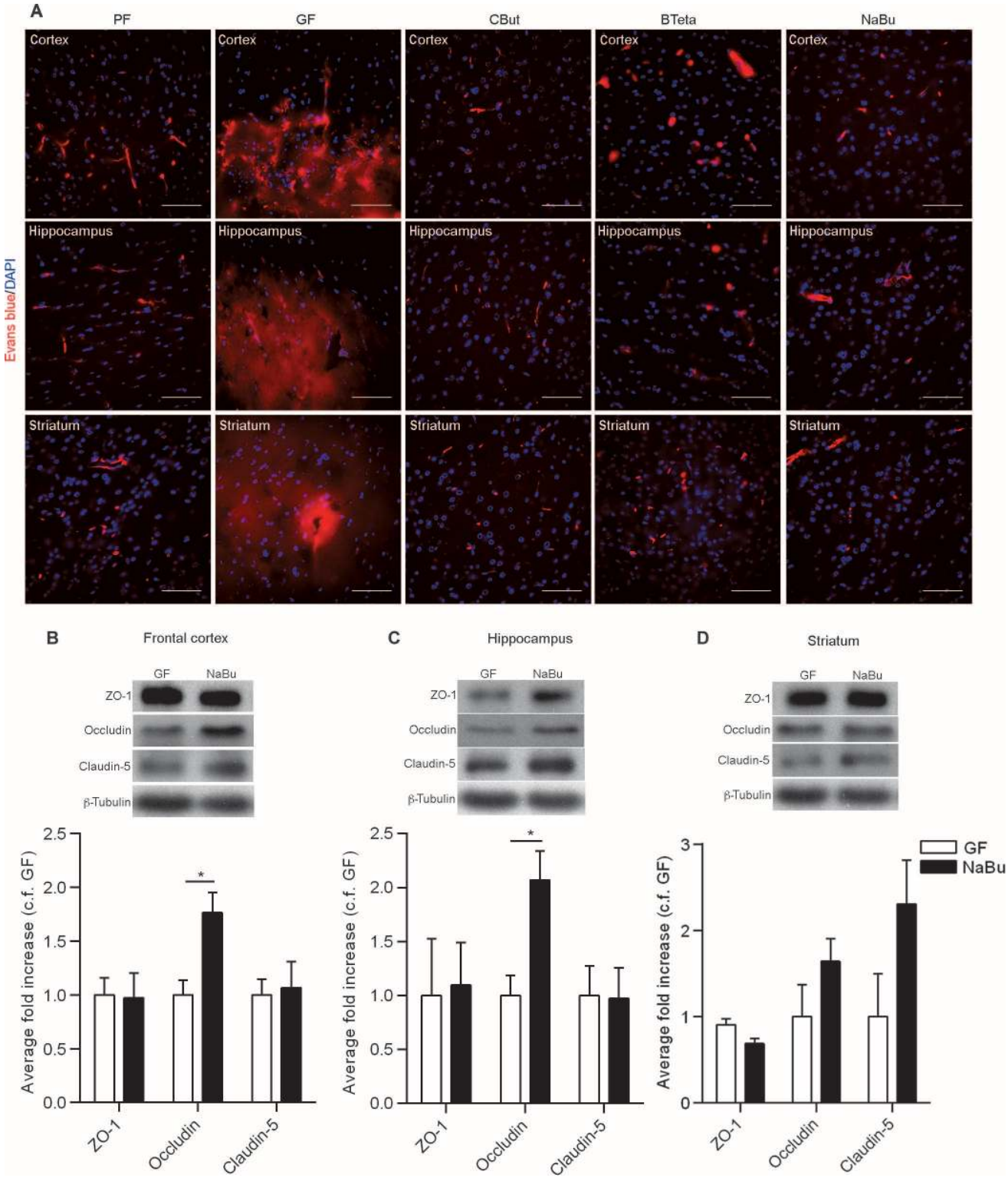


**Fig. 6. The effect of SCFAs on BBB permeability.** (**A**) Extravasation of Evans blue dye (red) observed in the brain regions (frontal cortex, striatum, and hippocampus) of germ-free (GF) mice. In germ-free mice monocolonized with either *C. tyrobutyricum* (CBut) or *B. thetaiotaomicron* (BTeta) for 2 weeks or mice treated with the bacterial metabolite sodium butyrate (NaBu) for 72 hours, Evans blue dye was detected only in the blood vessels, without any leakage into the brain parenchyma. Blue, DAPI (nuclear staining). Scale bars, 50 μm. (**B** to **D**) Quantitative analysis of ZO-1, occludin, and claudin-5 expression in brain lysates from germ-free mice gavaged with water (GF) or NaBu for 72 hours. Data were normalized for β-tubulin expression as a loading control and expressed as fold change, control fold (c.f.) GF. Values are expressed as means ± SEM (four to five mice per group). *$P < 0.05$ by Student's $t$ test compared to the germ-free control.

was similar to that in pathogen-free mice, suggesting that altering the number of pericytes is unlikely to account for the increased BBB permeability observed in germ-free mice. This is similar to the Mfsd2a-deficient mouse model in which leaky vessels are not associated with changes in the cerebrovascular network or pericyte abnormalities (*11*). However, in contrast to the Mfsd2a-deficient mouse where transcytosis across the BBB is affected without disruption of tight junctions, our model implies that the gut microbiota may regulate the BBB through modulation of tight junction protein expression.

Tight junctions play a major role in the functional maintenance of the BBB (*27*, *28*). Our data show disorganized tight junctions in the brains of germ-free adult mice compared with those of pathogen-free mice, which was associated with lower expression of occludin and claudin-5. No difference in the expression of ZO-1 was observed. A decrease in occludin and claudin-5 paralleled by cytoskeletal changes and tight junction protein redistribution was associated with altered integrity of the BBB (*29*). Reduced expression of occludin was observed in germ-free mice during both intrauterine life and adulthood and was associated with increased permeability of the BBB. Administration of normal flora from pathogen-free mice or oral treatment with the bacterial metabolite sodium butyrate to germ-free adult mice induced an increase in the expression of occludin that was associated with decreased permeability of the BBB. These observations imply that the expression of occludin by the brain endothelial cells is sensitive to changes in the intestinal gut microbiota.

Regulation of occludin expression by the intestinal microbiota has been reported in the intestinal epithelial barrier (*30*) and blood-testis barrier (*31*). The expression of claudin-5 by brain endothelial cells was low in germ-free adult mice but elevated after exposure to the gut microbiota. However, no difference in the expression of claudin-5 was observed in the E18.5 cortex of fetal mice with germ- or pathogen-free mothers. This implies that claudin-5 expression continues to increase during the postnatal period in offspring of pathogen-free mothers but not in offspring of germ-free mice. Although claudin-5 expression is present from early intrauterine life in the human brain, it is localized mostly in the endothelial cytoplasm and shifts toward the endothelial border during development to form tight junctions (*32*, *33*). Furthermore, claudin-5 knockout mice appear to develop normally during intrauterine life with morphologically normal blood vessels but have a BBB impairment associated with increased permeability to small molecules (*34*). The complete depletion of claudin-5 is associated with 100% mortality of the newborns within 10 hours of birth (*34*), further supporting the role of claudin-5 in the postnatal regulation of the BBB.

Dietary carbohydrates are substrates for fermentation by certain gut bacteria, which produce SCFAs, primarily acetate, propionate, and butyrate, as end products (*35*). These SCFAs have been shown to regulate intestinal motility (*36*, *37*) and to be involved in central appetite regulation (*38*, *39*) as well as being taken up directly into the bloodstream and transported to various organs, including the brain (*39*, *40*), where they modulate tissue development and function (*41*, *42*). Physiological concentrations of SCFA mixtures or individual SCFAs regulate intestinal barrier function by increasing the transepithelial electrical resistance and decreasing paracellular permeability (*43*). In a rat model of transient focal cerebral ischemia, intraperitoneally injected sodium butyrate attenuated BBB disruption (*6*). In our study, we show that monocolonization of the intestine of germ-free adult mice with either *C. tyrobutyricum*, a bacterial strain producing butyrate (*19*, *44*), or *B. thetaiotaomicron*, which produces mainly acetate and propionate (*21*), decreased BBB permeability. Oral administration of the bacterial metabolite sodium butyrate mimicked this effect on the BBB. The effects of the other metabolites, acetate and propionate, as single substrates may also have an effect on the permeability of the BBB and should also be explored. Intravenous or intraperitoneal administration of sodium butyrate has been reported to inhibit histone deacetylation and facilitate long-term memory consolidation (*45*), prevent BBB breakdown (*46*), and promote angiogenesis and neurogenesis (*47*, *48*). Whether the gut microbiota and sodium butyrate alter histone acetylation of brain microvascular endothelial cells requires further study to better understand the effects of SCFAs produced by the gut microbiota on the CNS. Cumulative and chronic exposure to SCFAs could lead to relatively stable effects on gene expression in the brain.

Finally, the composition and diversity of the gut microbiota community change over time, presumably reflecting different gut microbiota–host interactions. Early in life, there is an urgent need to support the growing offspring with an almost unlimited amount of energy to ensure brain development. Germ-free mice show an increase in glucocorticoid production due to metabolic stress (*49*). An increase in BBB permeability may, therefore, allow serum glucocorticoids to enter the growing brain, affecting neurogenesis and impairing production of brain-derived nerve growth factor in the brain (*6*). In addition, microbes regulating the BBB in infants with a growing brain may influence BBB permeability differently compared to the adult BBB (*50*).

Although providing a first glimpse into an additional layer of gut-brain communication, the current study has not revealed the precise signaling mechanisms through which gut microbiota modulates BBB function. In addition, the consequences of increased BBB permeability in germ-free mice on neuronal function throughout life are still not known. Therefore, the results should be interpreted cautiously until more physiological data are acquired to corroborate these findings.

## MATERIALS AND METHODS

### Study design

The objective of this study was to assess the importance of the intestinal microbiota in the maintenance of BBB integrity in a mouse model. The integrity of the BBB was examined in germ-free mice and in pathogen-free mice using functional permeability assays and by determining the status of tight junctions. BBB integrity was also determined in a group of germ-free adult mice colonized with fecal samples from pathogen-free adult mice or treated with bacterial strains that produced SCFAs or the bacterial metabolite sodium butyrate.

### Animals

Germ- and pathogen-free NMRI (Naval Medical Research Institute) male mice and C57BL/6J female and male mice (8 to 10 weeks old) (Core Facility for Germ-free Research, Karolinska Institutet) were used. C57BL/6J, Balb/c, and NMRI germ- and pathogen-free female mice undergoing timed pregnancies were used to assess the intrauterine development of the BBB. Germ-free mice were raised in special plastic isolators. All animals were maintained on autoclaved R36 Lactamin chow (Lactamin), given sterile drinking water ad libitum, and kept under 12-hour light/dark cycles.

The protocols were approved by the Regional Animal Research Ethical Board, Stockholm, Sweden, following the proceedings described in the (European Union) EU legislation (Council Directive 2010/63/EU) and the Institutional Animal Care and Use Committee at The Feinstein Institute for Medical Research, Manhasset, NY, USA.

### Colonization of germ-free mice

For colonization, 8- to 10-week-old C57BL/6J germ-free mice received fecal matter from the pathogen-free mice through a single gavage and then were left for 14 days (CONV) before being sacrificed. The control group was gavaged with sterile PBS.

*C. tyrobutyricum* (DSM 2637) (a contribution of H. Kozakova, Department of Immunology and Gnotobiology, Institute of Microbiology, Academy of Sciences of the Czech Republic, Praha, Czech Republic) and *B. thetaiotaomicron* (BTeta) were cultured in Bryant Burkey broth with resazurine (Merck), and $10^8$ bacteria were used to colonize each C57BL/6J germ-free adult male mouse as previously described (*19*). Fourteen days later, the mice were treated with Evans blue dye to assess the BBB permeability. Another group of germ-free male mice was gavaged for 3 days with sodium butyrate [1 g/kg body weight (BW) per day] before sacrifice. A group of germ-free male mice and another group of pathogen-free mice were gavaged with sterile water and used as controls.

### Drug treatment

A group of adult male pathogen-free mice receiving a single intravenous injection of TNFα (100 μg/kg BW) 15 hours before Evans blue perfusion were used as a positive control for a "leaky" BBB (*51*).

### Perfusion with Evans blue dye

Evans blue perfusion was performed as previously described (*52*). Briefly, anesthetized mice were perfused with PBS followed by Evans blue cocktail. Tissue cryosections were analyzed by fluorescence microscopy. A detailed description is provided in Supplementary Materials.

### In vivo PET imaging of [$^{11}$C]raclopride

Scans were performed in a microPET Focus 120 scanner (CTI Concorde Microsystems). The tracer (maximum volume, 200 μl) was administered by bolus injection via the tail vein into anesthetized mice. PET data were acquired in full three-dimensional mode, and images were reconstructed by standard two-dimensional filtered back projection using a ramp filter. The % SUV is the regional concentration of tissue radioactivity normalized for injected dose and BW. A complete description is provided in Supplementary Materials.

### R4A antibody injection and quantitative analysis

Germ- and pathogen-free adult male mice received intravenous injections of R4A dissolved in PBS. Forty-eight hours later, anesthetized mice were given transcardiac perfusion with 0.9% NaCl followed by 4% paraformaldehyde (PFA) (Histolab). Tissue cryosections stained with cresyl violet and neurons were sampled from comparable regions of the anterior dorsal hippocampus (*53*, *54*). A detailed protocol is provided in Supplementary Materials.

### Intravital two-photon laser scanning microscopy

TRITC-dextran (155 kD, Sigma) was injected retro-orbitally before imaging. Two-photon imaging was performed on a TriM Scope II (LaVision BioTec) equipped with an Olympus BX51 upright microscope fitted with a 20 × 0.95 numerical aperture water immersion objective and a Chameleon Ultra-II Tunable, Mode-locked Ti:Sapphire laser (Coherent) tuned to 880 nm for excitation of TRITC-dextran. Imaris (Bitplane) was used for three-dimensional image analysis. Volumetric index (VI), a parameter that indicates percentage of volume occupied by blood vessels within the analyzed *Z* stack, was calculated according to the following formula: VI = total blood vessel volume within the *Z* stack/total volume of the *Z* stack × 100.

### Immunofluorescence

Immunofluorescence was performed on 50-μm brain coronal cryotome sections blocked with 5% bovine serum albumin (BSA) (Sigma) and 0.5% Triton X-100 (Sigma) in PBS, followed by incubation with primary antibody as follows: rat anti-CD13 (BD Pharmingen, 558744), mouse anti-occludin (1:300, Invitrogen, 33-1500), mouse anti–claudin-5 (1:300, Invitrogen, 35-2500), and rabbit anti-laminin (1:400, Sigma, L9393). Sections were then incubated with secondary donkey anti-rat Alexa 488, goat anti-mouse Alexa 488, or goat anti-rabbit Alexa 594 (1:500, Invitrogen) for 1 hour at room temperature. *Z* stack images were visualized and acquired using a Nikon Eclipse TE300 inverted microscope integrated with a PerkinElmer UltraVIEW spinning disk confocal system. Image processing was done using Corel Paint Shop Pro Photo XI software.

### Protein extraction and Western blot analysis

Protein expression was determined in brain lysates as previously described (*19*). Primary antibodies (occludin: 1:1000, Invitrogen, 331500; claudin-5: 1:1000, Invitrogen, 352500; and ZO-1: 1:2000, Invitrogen, 617300) diluted in 3% BSA in 0.1% Tween 20 (Sigma)/PBS were incubated overnight at 4°C with the blot. Protein bands were visualized by chemiluminescence using Immun-Star WesternC chemiluminescence kit (Bio-Rad). Protein expression was then quantified using ImageJ software (National Institute of Mental Health).

### Transmission electron microscopy

A group of adult pathogen- and germ-free mice were transcardially perfused with 2.5% glutaraldehyde (Sigma)/1% PFA and processed for transmission electron microscopy. Digital images were taken with a Veleta camera (Olympus Soft Imaging Solutions, GmbH). The full method is described in Supplementary Materials.

### Statistical analysis

Statistical significance was determined using one-way ANOVA with Tukey post hoc test for multiple groups, Bonferroni post hoc analysis for Fig. 1B, or *t* test when changes were compared between two groups (GraphPad Prism 6). $P < 0.05$ was considered statistically significant unless otherwise stated. Values were expressed as means ± SEM.

## SUPPLEMENTARY MATERIALS

www.sciencetranslationalmedicine.org/cgi/content/full/6/263/263ra158/DC1

Material and Methods

Fig. S1. Expression of tight junction proteins in the brains of germ- and pathogen-free adult female mice.

Fig. S2. Electron micrographs showing different tight junction structure (white arrows) in the brains of germ-free adult mice.

Fig. S3. The effect of oral treatment with the bacterial metabolite sodium butyrate or monocolonization with *C. tyrobutyricum* on histone acetylation in extracts of mouse brain frontal cortex.

## REFERENCES AND NOTES

1. F. Bäckhed, R. E. Ley, J. L. Sonnenburg, D. A. Peterson, J. I. Gordon, Host-bacterial mutualism in the human intestine. *Science* **307**, 1915–1920 (2005).
2. L. V. Hooper, Bacterial contributions to mammalian gut development. *Trends Microbiol.* **12**, 129–134 (2004).
3. V. R. Velagapudi, R. Hezaveh, C. S. Reigstad, P. Gopalacharyulu, L. Yetukuri, S. Islam, J. Felin, R. Perkins, J. Borén, M. Oresic, F. Bäckhed, The gut microbiota modulates host energy and lipid metabolism in mice. *J. Lipid Res.* **51**, 1101–1112 (2010).

4. J. K. Nicholson, E. Holmes, J. Kinross, R. Burcelin, G. Gibson, W. Jia, S. Pettersson, Host-gut microbiota metabolic interactions. *Science* **336**, 1262–1267 (2012).
5. L. V. Hooper, D. R. Littman, A. J. Macpherson, Interactions between the microbiota and the immune system. *Science* **336**, 1268–1273 (2012).
6. R. Diaz Heijtz, S. Wang, F. Anuar, Y. Qian, B. Björkholm, A. Samuelsson, M. L. Hibberd, H. Forssberg, S. Pettersson, Normal gut microbiota modulates brain development and behavior. *Proc. Natl. Acad. Sci. U.S.A.* **108**, 3047–3052 (2011).
7. B. Engelhardt, Development of the blood-brain barrier. *Cell Tissue Res.* **314**, 119–129 (2003).
8. T. K. Hensch, Critical period regulation. *Annu. Rev. Neurosci.* **27**, 549–579 (2004).
9. E. I. Knudsen, Sensitive periods in the development of the brain and behavior. *J. Cogn. Neurosci.* **16**, 1412–1425 (2004).
10. R. Daneman, L. Zhou, A. A. Kebede, B. A. Barres, Pericytes are required for blood–brain barrier integrity during embryogenesis. *Nature* **468**, 562–566 (2010).
11. A. Ben-Zvi, B. Lacoste, E. Kur, B. J. Andreone, Y. Mayshar, H. Yan, C. Gu, Mfsd2a is critical for the formation and function of the blood–brain barrier. *Nature* **509**, 507–511 (2014).
12. B. T. Hawkins, T. P. Davis, The blood-brain barrier/neurovascular unit in health and disease. *Pharmacol. Rev.* **57**, 173–185 (2005).
13. C. Tscheik, I. E. Blasig, L. Winkler, Trends in drug delivery through tissue barriers containing tight junctions. *Tissue Barriers* **1**, e24565 (2013).
14. A. Armulik, G. Genové, M. Mäe, M. H. Nisancioglu, E. Wallgard, C. Niaudet, L. He, J. Norlin, P. Lindblom, K. Strittmatter, B. R. Johansson, C. Betsholtz, Pericytes regulate the blood–brain barrier. *Nature* **468**, 557–561 (2010).
15. E. Dejana, E. Tournier-Lasserve, B. M. Weinstein, The control of vascular integrity by endothelial cell junctions: Molecular basis and pathological implications. *Dev. Cell* **16**, 209–221 (2009).
16. J. M. Mariadason, D. H. Barkla, P. R. Gibson, Effect of short-chain fatty acids on paracellular permeability in Caco-2 intestinal epithelium model. *Am. J. Physiol.* **272**, G705–G712 (1997).
17. J. M. Mariadason, A. Catto-Smith, P. R. Gibson, Modulation of distal colonic epithelial barrier function by dietary fibre in normal rats. *Gut* **44**, 394–399 (1999).
18. L. Peng, Z. He, W. Chen, I. R. Holzman, J. Lin, Effects of butyrate on intestinal barrier function in a Caco-2 cell monolayer model of intestinal barrier. *Pediatr. Res.* **61**, 37–41 (2007).
19. A. Korecka, T. de Wouters, A. Cultrone, N. Lapaque, S. Pettersson, J. Doré, H. M. Blottière, V. Arulampalam, ANGPTL4 expression induced by butyrate and rosiglitazone in human intestinal epithelial cells utilizes independent pathways. *Am. J. Physiol. Gastrointest. Liver Physiol.* **304**, G1025–G1037 (2013).
20. P. Louis, H. J. Flint, Diversity, metabolism and microbial ecology of butyrate-producing bacteria from the human large intestine. *FEMS Microbiol. Lett.* **294**, 1–8 (2009).
21. J. Noack, G. Dongowski, L. Hartmann, M. Blaut, The human gut bacteria *Bacteroides thetaiotaomicron* and *Fusobacterium varium* produce putrescine and spermidine in cecum of pectin-fed gnotobiotic rats. *J. Nutr.* **130**, 1225–1231 (2000).
22. B. S. Samuel, J. I. Gordon, A humanized gnotobiotic mouse model of host–archaeal–bacterial mutualism. *Proc. Natl. Acad. Sci. U.S.A.* **103**, 10011–10016 (2006).
23. U. Kniesel, W. Risau, H. Wolburg, Development of blood-brain barrier tight junctions in the rat cortex. *Brain Res. Dev. Brain Res.* **96**, 229–240 (1996).
24. J. A. Siegenthaler, F. Sohet, R. Daneman, 'Sealing off the CNS': Cellular and molecular regulation of blood–brain barriergenesis. *Curr. Opin. Neurobiol.* **23**, 1057–1064 (2013).
25. O. Koren, J. K. Goodrich, T. C. Cullender, A. Spor, K. Laitinen, H. K. Bäckhed, A. Gonzalez, J. J. Werner, L. T. Angenent, R. Knight, F. Bäckhed, E. Isolauri, S. Salminen, R. E. Ley, Host remodeling of the gut microbiome and metabolic changes during pregnancy. *Cell* **150**, 470–480 (2012).
26. N. J. Abbott, A. A. Patabendige, D. E. Dolman, S. R. Yusof, D. J. Begley, Structure and function of the blood-brain barrier. *Neurobiol. Dis.* **37**, 13–25 (2010).
27. H. Jiao, Z. Wang, Y. Liu, P. Wang, Y. Xue, Specific role of tight junction proteins claudin-5, occludin, and ZO-1 of the blood–brain barrier in a focal cerebral ischemic insult. *J. Mol. Neurosci.* **44**, 130–139 (2011).
28. H. Wolburg, A. Lippoldt, Tight junctions of the blood–brain barrier: Development, composition and regulation. *Vascul. Pharmacol.* **38**, 323–337 (2002).
29. G. Schreibelt, G. Kooij, A. Reijerkerk, R. van Doorn, S. I. Gringhuis, S. van der Pol, B. B. Weksler, I. A. Romero, P. O. Couraud, J. Piontek, I. E. Blasig, C. D. Dijkstra, E. Ronken, H. E. de Vries, Reactive oxygen species alter brain endothelial tight junction dynamics via RhoA, PI3 kinase, and PKB signaling. *FASEB J.* **21**, 3666–3676 (2007).
30. P. D. Cani, S. Possemiers, T. Van de Wiele, Y. Guiot, A. Everard, O. Rottier, L. Geurts, D. Naslain, A. Neyrinck, D. M. Lambert, G. G. Muccioli, N. M. Delzenne, Changes in gut microbiota control inflammation in obese mice through a mechanism involving GLP-2-driven improvement of gut permeability. *Gut* **58**, 1091–1103 (2009).
31. M. Al-Asmakh, J. B. Stukenborg, A. Reda, F. Anuar, M. L. Strand, L. Hedin, S. Pettersson, O. Söder, The gut microbiota and developmental programming of the testis in mice. *PLOS One* **9**, e103809 (2014).
32. J. A. Anstrom, C. R. Thore, D. M. Moody, W. R. Brown, Immunolocalization of tight junction proteins in blood vessels in human germinal matrix and cortex. *Histochem. Cell Biol.* **127**, 205–213 (2007).
33. D. Virgintino, M. Errede, D. Robertson, C. Capobianco, F. Girolamo, A. Vimercati, M. Bertossi, L. Roncali, Immunolocalization of tight junction proteins in the adult and developing human brain. *Histochem. Cell Biol.* **122**, 51–59 (2004).
34. T. Nitta, M. Hata, S. Gotoh, Y. Seo, H. Sasaki, N. Hashimoto, M. Furuse, S. Tsukita, Size-selective loosening of the blood-brain barrier in claudin-5–deficient mice. *J. Cell Biol.* **161**, 653–660 (2003).
35. S. E. Pryde, S. H. Duncan, G. L. Hold, C. S. Stewart, H. J. Flint, The microbiology of butyrate formation in the human colon. *FEMS Microbiol. Lett.* **217**, 133–139 (2002).
36. P. S. Kamath, M. T. Hoepfner, S. F. Phillips, Short-chain fatty acids stimulate motility of the canine ileum. *Am. J. Physiol.* **253**, G427–G433 (1987).
37. A. Richardson, A. T. Delbridge, N. J. Brown, R. D. Rumsey, N. W. Read, Short chain fatty acids in the terminal ileum accelerate stomach to caecum transit time in the rat. *Gut* **32**, 266–269 (1991).
38. M. L. Sleeth, E. L. Thompson, H. E. Ford, S. E. Zac-Varghese, G. Frost, Free fatty acid receptor 2 and nutrient sensing: A proposed role for fibre, fermentable carbohydrates and short-chain fatty acids in appetite regulation. *Nutr. Res. Rev.* **23**, 135–145 (2010).
39. G. Frost, M. L. Sleeth, M. Sahuri-Arisoylu, B. Lizarbe, S. Cerdan, L. Brody, J. Anastasovska, S. Ghourab, M. Hankir, S. Zhang, D. Carling, J. R. Swann, G. Gibson, A. Viardot, D. Morrison, E. Louise Thomas, J. D. Bell, The short-chain fatty acid acetate reduces appetite via a central homeostatic mechanism. *Nat. Commun.* **5**, 3611 (2014).
40. F. De Vadder, P. Kovatcheva-Datchary, D. Goncalves, J. Vinera, C. Zitoun, A. Duchampt, F. Bäckhed, G. Mithieux, Microbiota-generated metabolites promote metabolic benefits via gut-brain neural circuits. *Cell* **156**, 84–96 (2014).
41. W. Scheppach, Effects of short chain fatty acids on gut morphology and function. *Gut* **35**, S35–S38 (1994).
42. D. F. Macfabe, Short-chain fatty acid fermentation products of the gut microbiome: Implications in autism spectrum disorders. *Microb. Ecol. Health Dis.* **23**, 19260 (2012).
43. T. Suzuki, S. Yoshida, H. Hara, Physiological concentrations of short-chain fatty acids immediately suppress colonic epithelial permeability. *Br. J. Nutr.* **100**, 297–305 (2008).
44. T. Hudcovic, J. Kolinska, J. Klepetar, R. Stepankova, T. Rezanka, D. Srutkova, M. Schwarzer, V. Erban, Z. Du, J. M. Wells, T. Hrncir, H. Tlaskalova-Hogenova, H. Kozakova, Protective effect of *Clostridium tyrobutyricum* in acute dextran sodium sulphate-induced colitis: Differential regulation of tumour necrosis factor-α and interleukin-18 in BALB/c and severe combined immunodeficiency mice. *Clin. Exp. Immunol.* **167**, 356–365 (2012).
45. J. M. Levenson, K. J. O'Riordan, K. D. Brown, M. A. Trinh, D. L. Molfese, J. D. Sweatt, Regulation of histone acetylation during memory formation in the hippocampus. *J. Biol. Chem.* **279**, 40545–40559 (2004).
46. E. B. Fessler, F. L. Chibane, Z. Wang, D. M. Chuang, Potential roles of HDAC inhibitors in mitigating ischemia-induced brain damage and facilitating endogenous regeneration and recovery. *Curr. Pharm. Des.* **19**, 5105–5120 (2013).
47. H. J. Kim, P. Leeds, D. M. Chuang, The HDAC inhibitor, sodium butyrate, stimulates neurogenesis in the ischemic brain. *J. Neurochem.* **110**, 1226–1240 (2009).
48. D. Y. Yoo, W. Kim, S. M. Nam, D. W. Kim, J. Y. Chung, S. Y. Choi, Y. S. Yoon, M. H. Won, I. K. Hwang, Synergistic effects of sodium butyrate, a histone deacetylase inhibitor, on increase of neurogenesis induced by pyridoxine and increase of neural proliferation in the mouse dentate gyrus. *Neurochem. Res.* **36**, 1850–1857 (2011).
49. N. Sudo, Y. Chida, Y. Aiba, J. Sonoda, N. Oyama, X. N. Yu, C. Kubo, Y. Koga, Postnatal microbial colonization programs the hypothalamic–pituitary–adrenal system for stress response in mice. *J. Physiol.* **558**, 263–275 (2004).
50. M. J. Claesson, I. B. Jeffery, S. Conde, S. E. Power, E. M. O'Connor, S. Cusack, H. M. Harris, M. Coakley, B. Lakshminarayanan, O. O'Sullivan, G. F. Fitzgerald, J. Deane, M. O'Connor, N. Harnedy, K. O'Connor, D. O'Mahony, D. van Sinderen, M. Wallace, L. Brennan, C. Stanton, J. R. Marchesi, A. P. Fitzgerald, F. Shanahan, C. Hill, R. P. Ross, P. W. O'Toole, Gut microbiota composition correlates with diet and health in the elderly. *Nature* **488**, 178–184 (2012).
51. M. Tsuge, K. Yasui, T. Ichiyawa, Y. Saito, Y. Nagaoka, M. Yashiro, N. Yamashita, T. Morishima, Increase of tumor necrosis factor-α in the blood induces early activation of matrix metalloproteinase-9 in the brain. *Microbiol. Immunol.* **54**, 417–424 (2010).
52. J. del Valle, A. Camins, M. Pallàs, J. Vilaplana, C. Pelegrí, A new method for determining blood–brain barrier integrity based on intracardiac perfusion of an Evans Blue–Hoechst cocktail. *J. Neurosci. Methods* **174**, 42–49 (2008).
53. C. Kowal, L. A. DeGiorgio, T. Nakaoka, H. Hetherington, P. T. Huerta, B. Diamond, B. T. Volpe, Cognition and immunity: Antibody impairs memory. *Immunity* **21**, 179–188 (2004).
54. B. T. Volpe, J. Wildmann, C. A. Altar, Brain-derived neurotrophic factor prevents the loss of nigral neurons induced by excitotoxic striatal-pallidal lesions. *Neuroscience* **83**, 741–748 (1998).


**Acknowledgments:** We thank V. Arulampalam and C. Betsholtz for their valuable comments. We thank A. Samuelsson, J. Aspsäter, and A. A. Bautista Amoyo for technical assistance. **Funding:** This project was supported by grants from Vetenskapsrådet, EU project "Molecular Targets Open for Regulation by the gut flora—New Avenues for improved Diet to Optimize European health," Hjärnfonden, Mérieux Institute, and Singapore Millennium Foundation and

funding from Lee Kong Chian School of Medicine, Nanyang Technological University to S.P. and grants from the NIH and the Simons Foundation to B.D. We also thank the Wenner-Gren Foundation for postdoctoral funding of V.B.; the Agency for Science, Technology and Research for the postdoctoral funding of F.A.; the Higher Education Institute and Qatar University for the Ph.D. funding of M.A.-A.; Karolinska Institutet doctoral funding for the Ph.D. scholarship to A.A.; and the Center for Innovative Medicine. **Author contributions:** V.B., F.A., B.D., and S.P. conceived of and designed the project. C.K. and M.A.-A. determined the permeability of the BBB in the fetal mice; M.T. performed the in vivo PET imaging; V.B., A.A., M.A.-A., and F.A. performed the Evans blue dye study; V.B. and B.T.V. performed the R4A injection and quantitative analysis; N.B. conducted the two-photon study; A.A. performed the immunofluorescence studies; V.B. performed the Western blot study for tight junction proteins, and F.A. performed the Western blot data for histone acetylation; K.H. and H.N. performed electron microscopy; and P.K. and M.A.-A. were involved in the animal experiments concerning the role of SCFAs. V.B., F.A., M.A.-A., C.K., M.T., B.T.V., N.B., L.G.N., B.D., A.K., and S.P. analyzed the data. V.B. and S.P. wrote the manuscript with significant input from B.G., C.H., L.G.N., C.K., H.H., M.A.-A., and B.D. **Competing interests:** The authors declare that they have no competing interests.

Submitted 11 June 2014
Accepted 31 October 2014
Published 19 November 2014
10.1126/scitranslmed.3009759

**Citation:** V. Braniste, M. Al-Asmakh, C. Kowal, F. Anuar, A. Abbaspour, M. Tóth, A. Korecka, N. Bakocevic, L. G. Ng, P. Kundu, B. Gulyás, C. Halldin, K. Hultenby, H. Nilsson, H. Hebert, B. T. Volpe, B. Diamond, S. Pettersson, The gut microbiota influences blood-brain barrier permeability in mice. *Sci. Transl. Med.* **6**, 263ra158 (2014).

Science Translational Medicine AAAS

**The gut microbiota influences blood-brain barrier permeability in mice**
Viorica Braniste *et al.*
*Sci Transl Med* **6**, 263ra158 (2014);
DOI: 10.1126/scitranslmed.3009759

Editor's Summary

## The Gut Microbiota and the Blood-Brain Barrier

The blood-brain barrier is an important gateway that controls the passage of molecules and nutrients in and out of the brain. An intact blood-brain barrier is a crucial checkpoint for appropriate development and function of the brain. Braniste *et al.* now show that germ-free pregnant dams, devoid of maternal microbes, have offspring that show increased permeability of the blood-brain barrier. This elevated permeability was also observed in adult germ-free mice. However, fecal transplants from mice exposed to bacteria into adult germ-free mice reduced blood-brain barrier permeability, possibly through the regulation of tight junction proteins. These findings suggest that crosstalk between the gut microbiota and the brain, initiated during the intrauterine period, is perpetuated throughout life.



*Science Translational Medicine* (print ISSN 1946-6234; online ISSN 1946-6242) is published weekly, except the last week in December, by the American Association for the Advancement of Science, 1200 New York Avenue NW, Washington, DC 20005. 